Contactless Biometric Based on Palm Vein Recognition Using Wavelet and Local Line Binary Patterns

Jayanti Yusmah Sari[1], Suharsono Bantun[2]
[1]Ilmu Komputer, Fakultas Teknologi Informasi, Universitas Sembilanbelas November Kolaka, Kolaka, Sulawesi Tenggara
[2]Sistem Informasi, Fakultas Teknologi Informasi, Universitas Sembilanbelas November Kolaka, Kolaka, Sulawesi Tenggara
[1]jayanti@usn.ac.id, [2]suharsonob@usn.ac.id

Abstract

Palm vein recognition has received much attention due to its advantages compared to other biometrics. Because it is contactless, this biometric system does not require physical contact between the user and the sensor device, thus providing several advantages in terms of comfort during acquisition and being more hygienic. In the palm vein recognition system, the palm vein pattern can be considered as a texture feature. Therefore, this study proposes a contactless biometric system based on palm vein recognition using the Local Line Binary Pattern method for extracting texture features of palm vein images resulting from the decomposition of 2D Wavelet Transformation, to produce a texture descriptor that is small and compatible with the texture characteristics of thin veins. The proposed texture feature extraction method has been tested using the Fuzzy k-NN classification method on 600 palm images with a CRR accuracy of 94.0% with a computation time of 0.057 seconds.

Keywords: contactless biometrics; fuzzy K-Nearest neighbor; local line binary patterns; palm vein; wavelet

1. Introduction

Biometrics or individual identity verification technology is often found in today's community activities, ranging from control systems, and recording attendance at offices/schools/agencies to access rights to a room. Generally, biometrics that are often used because they have high accuracy are fingerprint-based. However, the application of fingerprint-based biometrics requires the public to be in direct contact with sensors or scanners making this biometric unhygienic.

Since the early 2000s, research on palm vein recognition has been carried out to overcome the limitations in comfort and performance of other biometric recognition systems, such as fingerprint, face and iris recognition. The recognition of blood vessels in the palm, palm vein recognition, is contactless, that is, it does not require direct physical contact between the user and the sensor. Vein pattern images can be acquired without direct contact with the hand [1]. Compared to other biometric techniques, palm vein is difficult to fake or change because each person has unique patterns of veins [2] and veins are usually not visible to others [3]. Therefore, palm vein recognition provides several advantages in terms of convenience during acquisition, is more hygienic, and provides a low

risk of fake or theft. Contactless biometrics has been more prevalent over recent years due to the COVID-19 pandemic but has paved the way for more efficient and effective biometric systems for using palm veins to identify persons [4].

In the palm vein recognition system, the pattern of blood vessels can be considered as a texture feature. Texture feature extraction methods that have been used in palm vein recognition such as the Local Binary Pattern (LBP) [5],[6], Wavelet [7] - [9] and Adaptive Gabor filter [10] are not able to describe the characteristics of the vein image in the form of a thin texture, this can affect the level of accuracy produced [11]. One of the challenges in biometrics based on palm vein recognition is the characteristic of veins in the form of thin lines. For this reason, a reliable feature extraction method is needed to extract these vein features clearly so that the recognition process can be carried out accurately and of course without ignoring computation time. In this research, we build palm vein-based contactless biometrics that focus on the feature extraction stage to increase recognition accuracy and reduce computation time.

Local Line Binary Pattern (LLBP) is a variant of the LBP method [12]. The shape of the operator in the LLBP in the form of a line can extract thin vein features

better than the LBP operator in the form of a square [13], [14]. Therefore, in this study, the LLBP method will be used which is in accordance with the characteristics of the line features on the palm vein. However, because LLBP uses the basic concept of LBP, LLBP also produces a large texture descriptor, so it needs to be reduced so as not to increase the computing time of the system [15], [16]. The 2D Wavelet Transform is a method that can reduce the size of the image without removing important information from the image [7]. Therefore, in this study, the Local Line Binary Pattern method will be used to extract the texture features of the palm vein image from the decomposition of the 2D Wavelet Transform, so as to produce a texture descriptor that is small in size and by the characteristics of the thin vein texture.

This study aims to build contactless biometrics based on the recognition of palm vein with the following stages: dataset acquisition of blood vessels in the palm vein image, preprocessing, texture feature extraction, and classification method. As for the contribution of this study is on the feature extraction stage. We propose the Local Line Binary Pattern method for extracting texture features of palm vein images from the decomposition of 2D Wavelet Transform, to obtain a texture descriptor that is small in size and in accordance with the characteristics of thin palm vein texture. 2D Wavelet Transform is used to decompose the palm image so that the dimensions of the palm vein texture descriptor can be reduced first. The Local Line Binary Pattern (LLBP) is used to extract texture features in the form of veins in the palm vein image as a result of decomposition. And for classification step, we use the fuzzy k-NN [17] since it does not need any learning algorithm so that it can decrease the processing time [15]. In addition, due to the features of palm vein image that similar to each other, fuzzy k-NN method is choosen over SVM method [6] to avoid the false recognition of palm vein images. With promising result, this research is expected to produce alternative solutions for more efficient and effective contactless biometrics systems.

2. Research Methods

The proposed palm vein recognition system includes: 1) region of interest (ROI) detection, 2) preprocessing, 3) feature extraction using 2D Wavelet Transformation and Local Line Binary Pattern methods, and 4) palm vein image recognition based on features extracted using the Fuzzy *k*-Nearest Neighbor (FKNN) method.

Figure 1 shows a block diagram of the proposed palm vein recognition system, while the contribution of this research is in the highlighted section. We propose an authentication system that preserves the privacy of 2D Wavelet Transformation and Local Line Binary Pattern methods on feature extraction stage to improved accuracy and less computation time.
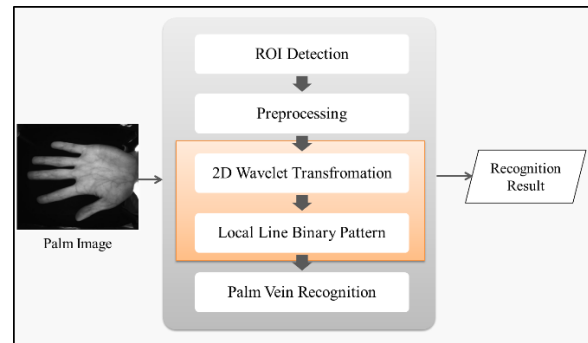

Figure 1. Block Diagram of Palm Vein Recognition System

2.1 Image Dataset

In this study, the left palm vein image was taken from 100 different people using a camera and electromagnetic spectrum lighting with a wavelength of 940nm (near infrared/NIR).

Figure 2. Sample of Palm Vein Image

Palm vein acquisition for each palm was carried out in two sessions over more than one month. In each session, 3 palm samples were taken for the same person using a near-infrared camera. Because it does not have position and posture restrictions, the palm shape of the resulting palm vein image has variations in size and rotation as shown in Figure 2. The palm vein dataset in this study is an 8-bit grey level, with a dimension is 768 x 576 pixels and in JPEG format. In the experiment, the dataset was divided into two parts, namely 500 images (5 samples for each person) for the database and 100 images (1 sample for each person) for data testing. In the system built, all datasets (both testing images and training images) will go through the region of interest (ROI) detection and preprocessing stages before going through the feature extraction stage.

2.2 Region of Interest (ROI) Detection

Before the preprocessing stage, it is necessary to detect ROI (region of interest) so that the extracted palm vein features come from the same part for each palm image. The ROI can eliminate irrelevant data (such as background interference), ROI greatly reduces the amount of computation for subsequent processing and reduces the influence of rotation and translation of the palm [18]. In this ROI detection stage, an anisotropic diffusion filter (ADF) [19], and image contour are used to get the interest point [20]. An example of ROI detection on a palm vein image is shown in Figure 3.

The image contour in Figure 3(a) has a similar concept to edge detection. However, the edges detected in the edge detection process are in the form of lines, while

the edges detected in the image contour process are curves. Because the detected edge is in the form of a curve an object area that contrasts with the background area can be obtained. From the contour image results obtained, the maximum contour image will be searched as shown in Figure 3(b).
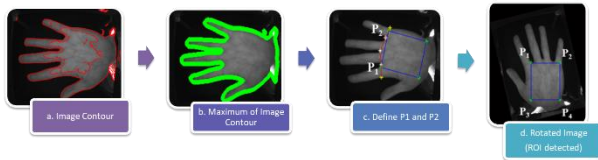

Figure 3. Sample of ROI Detection

The maximum image contour will produce a border that separates the palm area and the background area. From the maximum contour image, two interest points can be determined as shown in Figure 3. Interest points are reference points in ROI detection, namely points P_1 (between the index and middle fingers) and P_2 (between the ring finger and little finger). From these two points, a square area $P_1P_2P_3P_4$ can be formed with length P_1P_2 = length P_1P_3.

Although we employed two data points to find the ROI automatically in the previous step, there are still a few rotations during the detection of ROI. To eliminate the effect of rotational variations that occur during acquisition, the palm image will be rotated as shown in Figure 3(d), using the angle θ between the line $\overline{P_1P_2}$ and the horizontal line shown in Formula 1 [20].

$$\theta = \frac{tan^{-1}(Y_{P_2} - Y_{P_1})}{X_{P_2} - X_{P_1}} \tag{1}$$

(X_{P_1}, Y_{P_1}) and (X_{P_2}, Y_{P_2}) are the coordinates of points P_1 and P_2. The cropping process will be carried out on the $P_1P_2P_3P_4$ rectangular area from the rotated palm vein image and the result is stored as an ROI image of the palm vein with a size of I x J pixels. All stages of ROI detection in this study are shown in Figure 4. The ROI image will then become the input image in the preprocessing stage.
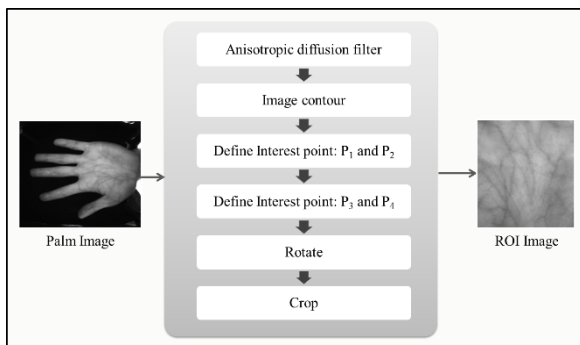

Figure 4. The Process of ROI Detection

2.3. Preprocessing

All preprocessing stags in this study are shown in Figure 5. All The images resulting from ROI detection will be resized to the same size 256 x 256 pixels using bicubic interpolation (Figure 5(a)). Noise removal and enhancement of a resized image are conducted using a median filter [21] with a kernel size of 10 x 10 and contrast-limited adaptive histogram equalization (CLAHE)adaptive histogram equalization and adaptive noise removal. The results are shown in Figures 5(b) and 5(c).

Furthermore, several steps were taken to separate the vein and background objects (palm), namely: 1) Anisotropic Diffusion Filter [19], 2) closing morphology operations, and 3) subtracting the Anisotropic Diffusion Filter (ADF) image with the resulting image of closing operation. The results of the three stages are shown in Figure 5(d), (e) and (f), respectively. In the final stage of the preprocessing, the image intensity value is improved (adjusting). The result of this stage as shown in Figure 5(g) is called a palm vein image because the vein part of the palm is quite visually clear. The preprocessed palm vein image is a grayscale image measuring 256 x 256 pixels. The palm vein image will then be the input image for each experiment in this study. The result of this stage is called the palm vein image because the vein part of the palm is quite visually clear. All preprocessing stages in this study are shown in Figure 5.
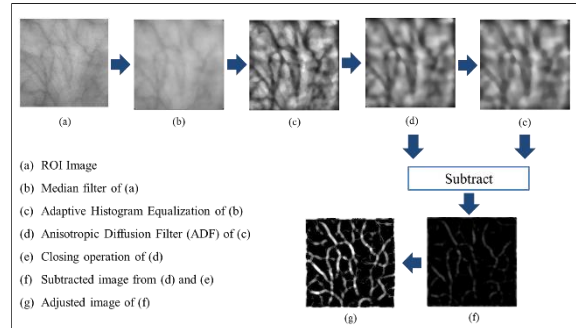

Figure 5. The Steps of Preprocessing

Figure 5(a) is an ROI image that will be preprocessed. The initial stage of the preprocessing is resizing the image size to 256 x 256 pixels using bicubic interpolation. Image noise removal is performed using a median filter with a kernel size of 10 x 10. The image resulting from the median filter is shown in Figure 5(b). The image enhancement process is carried out using contrast-limited adaptive histogram equalization (CLAHE). The results are shown in Figure 5(c).

Furthermore, several steps were conducted to separate vein and background objects (palms), namely: 1) Anisotropic Diffusion Filter [19], 2) closing morphology operations, and 3) subtracting (reducing) the image from the Anisotropic Diffusion Filter with the

image. result of closing operation. The results of the three stages are shown in Figure 5(d), (e) and (f), respectively. In the final stage of the preprocessing, the image intensity value is improved (adjusting).

2.4 Feature Extraction Using 2D Wavelet Transformation and Local Line Binary Pattern

The 2D Wavelet Transform method is used to decompose the preprocessed image of size M x M. M-level wavelet decomposition will produce one approximation image as shown in Figure 6(a) and 3 detailed images, namely vertical detail images as shown in Figure 6(b), horizontal detail image as shown in Figure 6(c) and diagonal detail image as shown in Figure 6(d).
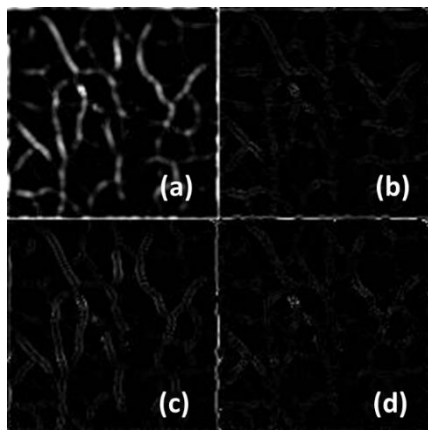

Figure 6. Sample of Decomposed Palm Vein Image Using 2D Wavelet Transformation

The dimension of four images from the decomposition is A x A, with $A = ½^k M$. In this study, an approximation image will be used (Figure 6(a)) for the feature extraction stage because, unlike the three detailed images that contain high frequencies, this approximation image contains low frequencies so that it can represent the features of the palm vein [22].

The image decomposition process using Wavelet transformation can be done by transforming each row of the image matrix, then continuing by transforming each column of the image matrix, both using a low pass filter and a high pass filter. Table 1 shows the scaling coefficient (low pass filter) and wavelet coefficient (high pass filter) for several types of wavelet filters.

The approximation image resulting from the wavelet decomposition will then be used for texture feature extraction using the Local Line Binary Pattern (LLBP) method. The LLBP operator consists of a horizontal component ($LLBP_h$) and a vertical component ($LLBP_v$). The magnitude value of LLBP is obtained by calculating the binary code of the two components using Formula 4. The LLBP operator is described in the Formula 2-6.

Table 1. Coefficients of Wavelet Filters [23]

Wavelet Filters	Coefficients	
	Low pass filter	High pass filter
Haar	0.7071	-0.7071
	0.7071	0.7071
Daubechies 2 (db2)	-0.1294	-0.4830
	0.2241	0.8365
	0.8365	-0.2241
	0.4830	-0.1294
Symlets 2 (sym2)	-0.1294	-0.4830
	0.2241	0.8365
	0.8365	-0.2241
	0.4830	-0.1294
Coiflets 1 (coif1)	-0.0157	0.0727
	-0.0727	0.3379
	0.3849	-0.8526
	0.8526	0.3849
	0.3379	0.0727
	-0.0727	-0.0157

$$LLBP_{hN,c}(x,y) = \sum_{n=1}^{c-1} s(h_n - h_c) \cdot 2^{c-n-1} + \sum_{n=c+1}^{N} s(h_n - h_c) \cdot 2^{c-n-1} \quad (2)$$

$$LLBP_{vN,c}(x,y) = \sum_{n=1}^{c-1} s(v_n - v_c) \cdot 2^{c-n-1} + \sum_{n=c+1}^{N} s(v_n - v_c) \cdot 2^{c-n-1} \quad (3)$$

$$LLBP_m = \sqrt{LLBP_h^2 + LLBP_v^2} \quad (4)$$

$$s(h_n - h_c) = \begin{cases} 1, & if\ h_n - h_c \geq 0 \\ 0, & if\ h_n - h_c < 0 \end{cases} \quad (5)$$

$$s(v_n - v_c) = \begin{cases} 1, & if\ v_n - v_c \geq 0 \\ 0, & if\ v_n - v_c < 0 \end{cases} \quad (6)$$

$LLBPh$, $LLBPv$ and $LLBPm$ are LLBP in the horizontal, vertical and magnitude directions, respectively. N is the length of the line in pixels, h_n is the pixel on the horizontal line and v_n is the pixel on the vertical line, $c = N/2$ is the position of the center pixcentreon the horizoon nhorizonand v_c on the vertical line, $s(h_n - h_c)$ and $s(v_n - v_c)$ defines the thresholding function as shown in Formulas 5 and 6 [23].

Using Formulas 2 and 3, the vertical line operator measuring N x 1 and the horizontal operator measuring 1 x N will generate binary codes ($LLBP_v$) and ($LLBP_h$) with sizes $N - 1$ for each pixel. The magnitude value ($LLBP_m$) of each pair of binary code vertical and horizontal pixels will be calculated using Formula 4 to obtain a palm vein texture descriptor.

The texture descriptor of the LLBP results is A x A with $A = 128$ for the approximation image resulting from the 1-level decomposition, $A = 64$ for the approximating image resulting from the 2nd-level decomposition, and $A = 32$ for the approximating image resulting from the 3rd level decomposition. Furthermore, the texture feature will be converted into a vector measuring 1 x AA and stored in the database as a texture feature for use in the test image recognition process. If there are several j images, then the resulting database is a matrix of size j x AA.

2.5 Classification Using Fuzzy *k*-Nearest Neighbour

Palm vein recognition is done by matching the texture features of the palm vein on the testing image and the texture features of the palm vein on the database image using the Fuzzy k-nearest Neighbor (FKNN) method. The FKNN method is used in this study because it does not require a learning algorithm so that it can optimize computational time [17].

3. Results and Discussions

To evaluate the palm vein recognition system thwasroposedanentification testing is conducted, namely one-to-many testing, each testing image is matched with all database images and then the accuracy of the recognition of all testing images will be calculated [20]. In the identification testing, the system is evaluated using CRR (correct recognition rate). The testing process is carried out on all palm vein images, by matching the test image with the database image. Accuracy is obtained by counting the number of correct recognition images from testing data.

The testing process was conducted on 600 palm vein images, by matching 100 testing images with 500 database images. Matching the testing image and the database image is done using the Fuzzy k-NN method. CRR recognition accuracy is obtained by calculating the ratio of the number of correct image recognition test data with the total number of test data. The accuracy results obtained will be validated using the *k*-fold cross-validation procedure with *k*=6 because there are 6 sample images for each palm. From the *k*-fold cross-validation procedure used, the mean accuracy is obtained for each test result.

In the experiment stage, computational time measurements were also carried out to measure the performance of the system that had been built. The computational time obtained in this study is the total computation time for the recognition of the entire image (100 test images).

There are several experiments conducted in this study to analyze the optimal parameters for the proposed method, namely the *m* parameter (*m*=1, 2 and 3) in the 2D Wavelet Transform which shows the number of decomposition levels, the *N* parameter (*N* = 7, 9, 11, 13, 15 and 17 [24]) in the Local Line Binary Pattern method which shows the number of neighbouring pixels used in this research, vertical and horizontal operators, the type of wavelet filter that produces the best accuracy, and the parameter *k* (*k*=2, 3, 4, 5, and 6) in the fuzzy *k*-NN method which shows the number of closest neighbours that are considered during the recognition process.

3.1 Result of *m* parameter in the 2D Wavelet Transform

At this stage, an experiment is conducted on the parameter *m* which shows the level of decomposition of

the 2D Wavelet Transform. The greater the value of *m*, the higher the decomposition level, the resulting features are smaller so they are processed more quickly by the system.

The image used as input is the approximation image of the decomposition result (Figure 6(a)). The purpose of this experiment is to obtain the optimal value of *m*. There are three *m* parameter values used in this trial, namely *m*=1, *m*=2 and *m*=3.
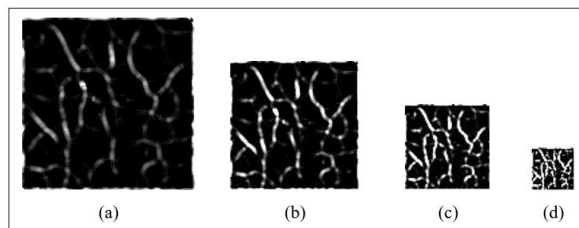

Figure 7. (a) preprocessed image, (b) *m*=1 decomposed image, (c) *m*=2 decomposed image and (d) hasil *m*=3 decomposed image

Figure 7 shows an example of a 2D Wavelet Transform decomposition for each *m* level using a Haar Wavelet filter. Figure 7(a) is a preprocessed palm vein image measuring 256 x 256 pixels, the image is the input image that will be processed in this experiment. Figure 7(b) is a 1-level decomposition image with 128 x 128 pixels, Figure 7(c) is a 2-level decomposition image with 64 x 64 pixels and Figure 7(d) is a 32 x 32 pixel 3-level decomposition image. After obtaining the image from the decomposition, classification is conducted to obtain accuracy and computational time for each *m* level of decomposition as shown in Table 2.

Table 2. Result of classification with *m-level* decomposition of Wavelet

m Level	Image size (pixel)	Feature size	Accuracy (%)	Time (s)
1	128 x 128	16384	82.7	65.49
2	64 x 64	4096	85.3	19.05
3	32 x 32	1024	91.8	8.31

From Table 2, it can be seen that the highest average accuracy reaches 91.8% at the 3rd level decomposition and the lowest reaches 82.7% at the 1st level decomposition. The fastest computational time reaches 8.31 seconds for the 3rd level decomposition and the longest computational time reaches 65.49 seconds for the 1st level decomposition.

From all decomposition level experiments, the 3rd level has the highest average accuracy compared to the 1st level and the 2nd level. This is because, at each level of decomposition of the Wavelet Transform, pixels are removed at high frequencies that contain noise that can affect the average accuracy. In addition, from this experiment, it was also found that the 3rd level decomposition has the fastest computational time compared to the 1st level and the 2nd level. This is because at the 3rd level decomposition, smaller features

(32 x 32) are produced compared to the 1st level decomposition (128 x 128) and the 2nd level (64 x 64). Based on the average accuracy and computational time obtained in this study, the 3rd level is considered the most optimal level for palm vein image decomposition before the feature extraction stage is carried out.

3.2 Result of N Neighborhood Pixel of LLBP

In this experiment, the input image used is an approximation image of the results of m levels (m = 1, 2, 3) in 2D Wavelet Transformation decomposition using the Haar filter. From the decomposition results, we get an approximation image with a size of 128 x 128 pixels for the 1st level decomposition, 64 x 64 pixels for the 2nd level decomposition and 32 x 32 pixels for the 3rd level decomposition. Each approximation image resulting from m-th levels of decomposition will then be extracted using the LLBP method with 6 different N values (N = 7, 9, 11, 13, 15 and 17) [24]. The texture features of the testing image generated in this experiment will be matched with the texture features in the database using Fuzzy k-NN with k = 2. The purpose of this experiment is to obtain optimal m and N parameters for palm vein recognition.

Table 3 shows the mean accuracy of the testing results for palm vein image recognition for each m level of decomposition and N number of neighbouring pixels. Figure 8 shows the computational time on the results of the palm vein image recognition for each m-th level of decomposition and N the number of neighbourhood pixels.

Table 3. Result of classification with N value of LLBP

m	Mean accuracy (%)					
	N=7	N=9	N=11	N=13	N=15	N=17
1	93.50	93.50	93.50	93.50	93.50	93.50
2	93.83	93.83	93.83	93.83	93.83	93.83
3	93.83	93.83	94.00	94.00	94.00	94.00

From Table 3, it can be seen that the highest average accuracy value, which is 94.00%, was obtained in the recognition of palm vein imagery from 3-level decomposition with N=11, N=13, N=15 and N=17. From the four different N values, N=11 was chosen as the optimal parameter because based on Figure 8, among the four N values, the shortest computational time was obtained at N=11. Therefore, the values of m=3 and N =11 are considered optimal values for the parameters m and N in this experiment. From Figure 8, it can be seen that the shortest average computational time (6.22 seconds) in the recognition of palm vein images results from 3rd-level decomposition. The combination of m=3 values for the decomposition level of 2D Wavelet Transform and N=11 for the number of LLBP neighboring pixels which produces an average of the highest average accuracy (94.00%) will be used in the next experiment.

Furthermore, Table 3 shows that the parameter N which is the number of neighboring pixels does not have a large influence on the average accuracy of palm vein recognition in this study. For each N value at each decomposition level, the difference in the average accuracy produced is less significant, ranging from 0-0.17%. In addition, Table 2 also shows that there is a less significant difference in average accuracy from 93.50% at the 1st level to 94.0% at the 3rd level. Thus, it can be concluded that the parameter m, which is the decomposition level of 2D Wavelet Transformation, does not have a significant effect. The average accuracy of palm vein recognition in this study is only 0.5%.
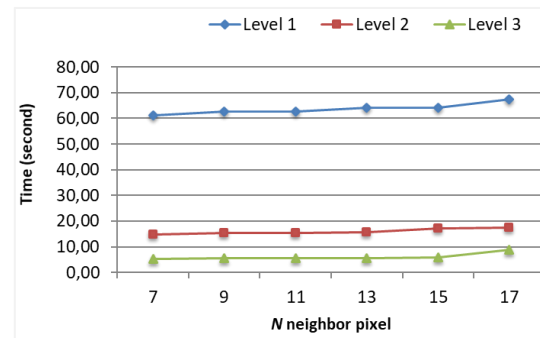

Figure 8. Computational Time of m Level and N Neighbor Pixel

Figure 8 shows that the fastest computational time reaches 5.44 seconds for the 3rd level decomposition with N=7 while the longest computational time reaches 67.47 seconds for the 1st level decomposition with N=17. For each level of decomposition, the average computational time is obtained with a significant difference, that is 63.70 seconds at the 1st level, 16.04 seconds at the 2nd level and 6.22 seconds at the 3rd level decomposition. Recognition of palm vein at the 3rd level has a computational time of 10 times faster when compared to the computational time on the 1st level. Thus, it can be concluded that the m parameter influences on the computation time. This is because the value of the parameter m indicates the number of levels in the image decomposition process. The larger the value of m, the smaller the size of the resulting image features to speed up computation time. Meanwhile, for each N value at each decomposition level, the difference in computational time is less significant, only ranging from 1-3 seconds, this can also be seen in Figure 8.

3.3 Results of Wavelet Filter Type

In this experiment, a combination of m=3 levels will be used for the decomposition of the 2D Wavelet Transform and N=11 for the number of LLBP neighbourhood pixels. This parameter value produces the highest average accuracy in the previous experiment using the Haar Wavelet filter. In this experiment, the mean accuracy of the results from the previous experiment using the Haar Wavelet filter will be compared with 3 other types of Wavelet filters, namely

Daubechies 2, Symlets 2 and Coiflets 1. The purpose of this experiment is to find the optimal Wavelet filter in the system of palm vein recognition. Therefore, in addition to accuracy (shown in Table 4), this experiment also evaluates and analyzes the computational time for each type of wavelet filter as shown in Figure 9.

Table 4. The accuracy of Wavelet Filter: Haar, Daubechies2, Symlets2 and Coiflets1

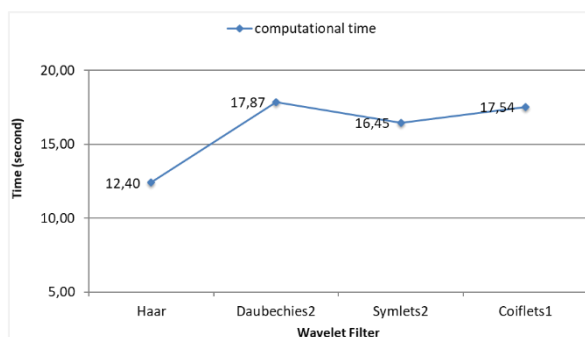| K-Fold	Accuracy (%)			
	Haar	Daubechies2	Symlets2	Coiflets1
1	95.0	91.0	91.0	93.0
2	94.0	91.0	91.0	92.0
3	93.0	92.0	92.0	91.0
4	95.0	92.0	92.0	94.0
5	94.0	95.0	95.0	95.0
6	93.0	94.0	94.0	93.0
Mean (%)	94.0	92.5	92.5	93.0

Figure 9. Computational Time of Wavelet Filter: Haar, Daubechies2, Symlets2 and Coiflets1

As shown in Table 4, the highest average accuracy obtained from this experiment reached 94.0% for the Haar Wavelet filter and the lowest average accuracy reached 92.5% for the Daubechies 2 and Symlets 2 Wavelet filters. This is because the Haar Wavelet filter has less effect on the decomposed image when compared to the other three Wavelet filters. As shown in Figure 10(b), the visualization of the texture features of the decomposed palm vein image using the Haar Wavelet filter is the most similar to the input image before decomposition.

In Figure 9, it can be seen the Haar Wavelet filter has the lowest computation time of 12.40 seconds compared to other Wavelet filters, which is 17.78 seconds for Daubechies 2, 16.45 seconds for Symlets 2, and 17.54 seconds for Coiflets 1. This is because the Haar Wavelet filter has the fewest coefficients of the other 3 Wavelet filters, which are 2 low pass filters and 2 high pass filters (See Table 1). The fewer Wavelet filter coefficients that are processed, the faster the computation time. With the results of this fastest computing time, the Wavelet Haar filter was used to decompose the palm vein image before the feature extraction stage.
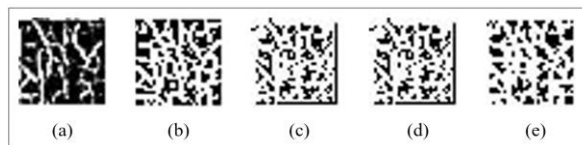

Figure 10. Sample of palm vein texture feature (a), Haar (b), Daubechies2 (c), Symlets2 (d), and Coiflets1 (e)

3.4 Result of k value of Fuzzy k-NN

In this experiment, the optimal parameters will be used, namely m=3 and N=11 and the Wavelet Haar filter which produces the best average accuracy in the previous experiment. The purpose of this experiment is to determine the effect of parameter k on the Fuzzy k-NN method on the accuracy of palm vein recognition. In the previous experiment, k=2 was used for the Fuzzy k-NN method. In this experiment, each feature of the palm vein test image will be matched with features in the database using Fuzzy k-NN with different k values, namely k = 3, 4, 5 and 6. The accuracy results of this experiment will be compared with the previous testing results. The results of this experiment are shown in Table 4.

Table 4. Result of k value of Fuzzy k-NN

K-Fold	Accuracy (%)				
	k=2	k=3	k=4	k=5	k=6
1	95.0	95.0	95.0	94.0	92.0
2	94.0	93.0	93.0	93.0	92.0
3	93.0	93.0	92.0	90.0	90.0
4	95.0	95.0	95.0	93.0	93.0
5	94.0	94.0	95.0	95.0	95.0
6	93.0	93.0	92.0	92.0	90.0
Mean (%)	94.0	93.83	93.67	92.83	92.0

As can be seen in Table 4, the highest mean accuracy value reached 94.0% at k=2, and the lowest average accuracy reached 92.0% with k=6. This does not mean that the value of k=2 is better than k=3, 4, 5 or 6. The results of this experiment only show that the value of k that is suitable for the data in this study is k=2. Therefore, for further experiments in this study, the value of k=2 for the Fuzzy k-NN method will be used.

3.5 Result of Proposed Method

This section discusses the comparison of the results of the proposed method with the previous method, namely the Local Binary Pattern (LBP). The LBP method can extract texture features on palm vein recognition quite well, but the resulting texture descriptor is large so it has a long computation time. In addition, the resulting texture descriptor is also not by the characteristics of thin palm vein texture features so it can affect the accuracy of palm vein recognition. In addition to the comparison with the LBP method, an evaluation of the performance of the proposed method was also carried out by comparing it with the combined performance of the 2D Wavelet Transform and LBP methods. In this experiment, the same testing data was used for methods

1) Wavelet, 2) LBP, 3) Wavelet + LBP, 4) LLBP and 5) Wavelet + LLBP. A comparison of the accuracy of the proposed method (method 5) with previous methods (methods 1-4) is shown in Figure 11.
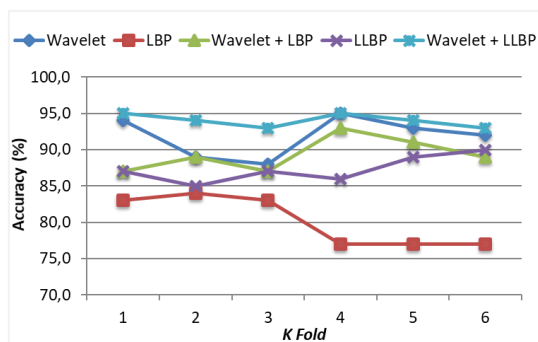

Figure 11. Accuracy of the proposed method and the previous method

From Figure 11 it can be seen that the 2D Wavelet Transform method has a higher average accuracy than LBP and LLBP. Furthermore, by combining 2D Wavelet Transformations with LBP and 2D Wavelet Transformations with LLBP, it is obtained that the average accuracy for combining 2D Wavelet Transformations with LLBP (94.0%) is higher than for combining 2D Wavelet Transformations with LBP (89.3%). This is because when compared to LBP operators in the form of square boxes, operators in LLBP in the form of vertical and horizontal lines are better able to describe the texture of the palm vein which has thin characteristics.

When compared with the previous method, the proposed method, which combines 2D Wavelet Transform with Haar filter and Local Line Binary Pattern (LLBP), has the highest average recognition accuracy reaching 95.0%. The other four methods, namely the 2D Wavelet Transformation method with Haar filter has an average accuracy of 91.8%, the combination of the 2D Wavelet Transformation method with Haar filter and Local Binary Pattern (LBP) has an average accuracy of 89.3%, the LLBP method has an average accuracy of 89.3%. the average accuracy is 87.3% and the last LBP method has an average accuracy of 80.2%. Thus, the proposed method can result in an average accuracy increase of 134.8% compared to the LBP method, ie from 80.2% to 94.0% in palm vein recognition. This is because, at each level of the Wavelet Transform decomposition in this study, there is a process of eliminating pixels at high frequencies that contain noise that can affect accuracy.

The comparison of the computational time between the proposed method and the previous method is shown in Figure 12. From Figure 12, it can be seen that with the proposed method, which is the combination of the 2D Wavelet Transform method and the LBP method, a significant change in computation time is obtained,

from 252.6 seconds when using the LLBP method only, to 5.7 seconds when using the 2D Wavelet Transform and LLBP methods. This is because with the decomposition process using 2D Wavelet Transform, the size of the image descriptor can be reduced to a smaller size to reduce computation time.
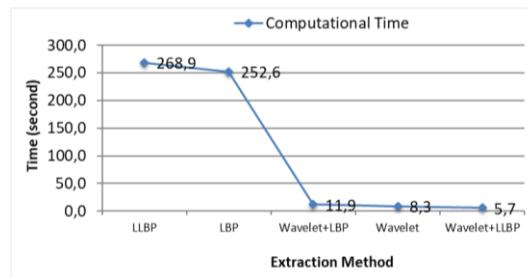

Figure 12. Computational Time of the proposed method and the previous method

Although the size of the image descriptor is smaller, the average recognition accuracy does not decrease, this is because the image used is an approximation image resulting from the decomposition of 2D Wavelet Transform. 2D Wavelet Transform Decomposition produces one approximation image and three detail images (Figure 6). The three detailed images resulting from the decomposition of 2D Wavelet Transform are vertical, horizontal and diagonal detailed images containing high-frequency pixels. While in the approximation image, the high-frequency palm vein image pixels containing local information have been removed. These pixels can be in the form of noise which can affect the recognition accuracy.

Thus, it can be concluded that the proposed method, which combines 2D Wavelet Transformation and Local Line Binary Pattern (LLBP) methods, can extract texture features on palm vein images well, with an average accuracy of 94.0% and a computation time of 0.057 seconds (5.7 seconds for 100 test images). This is because the combination of the two methods can produce an image descriptor that is small in size and according to the characteristics of a thin palm vein texture.

3.6 False Recognition

From experiments conducted, there were errors in the recognition of palm veins caused by errors at the ROI detection stage and the presence of pseudo features generated at the feature extraction stage. ?OI detection errors are caused by translational and rotational variations in the palm image dataset. The position and posture of the palms during dataset image acquisition thhaveoundarieso the palm shape of the resulting palm vein image hahaveranslational and rotational variations. The ROI detection method in this study has not been able to overcome many rotational and translational variations in the image dataset. The pseudo features or false features are the edges of the ROI image which are

considered asature veins after the feature extraction results. Similar to the previous palm vein research [11], [20], the texture features of the palm vein in this study are also influenced by the ROI margins which form pseudo features (the edges of the image which are considered as veins) of the palm vein image which can affect accuracy.

4. Conclusion

The proposed method in this study that combined 2D Wavelet Transform and Local Line Binary Pattern (LLBP) are capable of extracting texture features on palm vein images with an average accuracy of 94.0% and a computation time of 0.057 seconds, this is because the combination of the two methods can produce an image descriptor that is small in size and compatible with the characteristics of a thin palm vein texture. For further research, the authors suggest that the image ROI detection method used must be adaptive to translational and rotational variations in the palm vein image dataset to overcome ROI detection errors, in addition, the development of the Local Line Binary Pattern method to overcome the problem of pseudo texture features originating from the edge palm vein image is needed.

Acknowledgment

References

[1] D. Thapar, G. Jaswal, A. Nigam, and V. Kanhangad, "PVSNet: Palm vein authentication siamese network trained using triplet loss and adaptive hard mining by learning enforced domain specific features," in *2019 IEEE 5th international conference on identity, security, and behavior analysis (ISBA)*, 2019, pp. 1–8.

[2] H. I. Abdulrazzaq and R. D. Al-Dabbagh, "Biometric Identification System Based on Contactless Palm-Vein Using Residual Attention Network," *Iraqi J. Sci.*, pp. 1802–1810, 2022.

[3] E. Safronova and E. Pavelyeva, "Unsupervised Palm Vein Image Segmentation," in *CEUR Workshop Proceedings*, 2020, vol. 2744, pp. 1–12.

[4] R. Duggal, A. Pandya, and N. Gupta, "Deep Learning based Contactless Biometric Recognition using Bracelet Lines," in *2023 IEEE 8th International Conference for Convergence in Technology (I2CT)*, 2023, pp. 1–9.

[5] D. Fronitasari and D. Gunawan, "Palm vein recognition by using modified of local binary pattern (LBP) for extraction feature," in *2017 15th International Conference on Quality in Research (QiR): International Symposium on Electrical and Computer Engineering*, 2017, pp. 18–22.

[6] V. Ponnusamy, A. Sridhar, A. Baalaaji, and M. Sangeetha, "A palm vein recognition system based on a support vector machine," *IEEE Trans. Smart Process. Comput.*, vol. 8, no. 1, pp. 1–7, 2019.

[7] M. Wulandari, Basari, and D. Gunawan, "Evaluation of wavelet transform preprocessing with deep learning aimed at palm vein recognition application," in *AIP Conference Proceedings*, 2019, vol. 2193, no. 1, p. 50005.

[8] S. Visa, B. Ramsay, A. Ralescu, and E. van der Knaap, "Confusion Matrix-based Feature Selection Sofia," in *Proceeding of the 22nd Midwest Artificial Intelligence and Cognitive Science Conference*, 2011, vol. 710, pp. 120–127.

[9] W. Wu *et al.*, "Outside Box and Contactless Palm Vein Recognition Based on a Wavelet Denoising ResNet," *IEEE Access*, vol. 9, pp. 82471–82484, 2021.

[10] X. Ma, X. Jing, H. Huang, Y. Cui, and J. Mu, "Palm vein recognition scheme based on an adaptive Gabor filter," *Iet Biometrics*, vol. 6, no. 5, pp. 325–333, 2017.

[11] W. Kang and Q. Wu, "Contactless palm vein recognition using a mutual foreground-based local binary pattern," *IEEE Trans. Inf. Forensics Secur.*, vol. 9, no. 11, pp. 1974–1985, 2014.

[12] A. Petpon and S. Srisuk, "Face recognition with local line binary pattern," *Proc. 5th Int. Conf. Image Graph. ICIG 2009*, no. September, pp. 533–539, 2009, doi: 10.1109/ICIG.2009.123.

[13] A. Achban, H. A. Nugroho, and P. Nugroho, "Wrist hand vein recognition using local line binary pattern (LLBP)," in *2019 5th International Conference on Science and Technology (ICST)*, 2019, vol. 1, pp. 1–6.

[14] R. Malutan and S. Emerich, "Local Line Binary Pattern Vein Extraction from Dorsal Hand Images for Intruder Detection," in *2019 E-Health and Bioengineering Conference (EHB)*, 2019, pp. 1–4.

[15] J. Y. Sari, C. Fatichah, and N. Suciati, "Local Line Binary Pattern for Feature Extraction on Palm Vein Recognition," *J. Ilmu Komput. dan Inf.*, vol. 8, no. 2, pp. 111–118, Aug. 2015, doi: http://dx.doi.org/10.21609/jiki.v8i2.309.

[16] K. F. H. Holle, J. Y. Sari, and Y. P. Pasrun, "Local line binary pattern and Fuzzy K-NN for palm vein recognition," *J. Theor. Appl. Inf. Technol.*, vol. 95, no. 13, 2017.

[17] J. M. Keller, M. R. Gray, and J. A. G. JR, "A fuzzy k-nearest neighbor algorithm," *IEEE Trans. Syst. Man. Cybern.*, vol. (4), pp. 580–585, 1985.

[18] W. Wu, S. J. Elliott, S. Lin, and W. Yuan, "Low-cost biometric recognition system based on NIR palm vein image," *IET Biometrics*, vol. 8, no. 3, pp. 206–214, 2019.

[19] P. Perona and J. Malik, "Scale-Space and Edge Detection Using Anisotropic Diffusion," *IEEE Trans. Pattern Anal. Mach. Intell.*, vol. 12, no. 7, pp. 629–639, 1990, doi: 10.1109/34.56205.

[20] J.-C. Lee, "A novel biometric system based on palm vein image," *Pattern Recognit. Lett.*, vol. 33, no. 12, pp. 1520–1528, 2012.

[21] S. Rastogi, S. P. Duttagupta, A. Guha, and S. Prakash, "NIR Palm Vein Pattern Recognition," in *2020 IEEE International Conference for Innovation in Technology (INOCON)*, 2020, pp. 1–5.

[22] Q. Li, Y. Zeng, and K. Yang, "WAVELET-BASED PALM VEIN RECOGNITION SYSTEM," *J. Innov. Opt. Health Sci.*, vol. 3, no. 02, pp. 131–134, 2010.

[23] P. Getreuer, "Filter coefficients to popular wavelets," *MATLAB Cent.*, 2006.

[24] B. A. Rosdi, C. W. Shing, and S. A. Suandi, "Finger vein recognition using local line binary pattern," *Sensors*, vol. 11, no. 12, pp. 11357–11371, 2011.